INSTITUTE OF PHYSICS PUBLISHING JOURNAL OF PHYSICS: CONDENSED MATTER

J. Phys.: Condens. Matter **15** (2003) S2679–S2692 PII: S0953-8984(03)65316-6

# Electronic properties of interfaces between perylene derivatives and GaAs(001) surfaces

**T U Kampen[1,5], G Gavrila[1], H Méndez[1], D R T Zahn[1], A R Vearey-Roberts[2], D A Evans[2], J Wells[3], I McGovern[3] and W Braun[4]**

[1] Institut für Physik, Technische Universität Chemnitz, D-09107 Chemnitz, Germany
[2] Department of Physics, University of Wales, Aberystwyth SY23 3BZ, UK
[3] Physics Department, Trinity College, Dublin-2, Republic of Ireland
[4] BESSY GmbH, Albert-Einstein-Straße 15, D-12489 Berlin-Adlershof, Germany

E-mail: kampen@physik.tu-chemnitz.de

Received 26 June 2003
Published 12 September 2003
Online at stacks.iop.org/JPhysCM/15/S2679

**Abstract**

The adsorption of 3,4,9,10-perylenetetracarboxylic dianhydride (PTCDA) and *N*,*N*′-dimethyl-3,4,9,10-perylenetetracarboxylic diimide (DiMe-PTCDI) on differently treated n-doped GaAs(100) surfaces was investigated using high-resolution photoemission spectroscopy. The chemical interaction between the molecules and the semiconductor substrate is found to be weak; core level photoemission spectra show no additional chemically shifted peaks, indicating the absence of any covalent/ionic bond formation. Only a sharpening of the core level spectra is observed for a coverage lower than one monolayer and this is attributed to a reduction of inhomogeneous band bending at the surface. This is interpreted in terms of preferential sticking of the organic molecules to surface defects. The energy offset between the occupied states in the substrate and the organic film is directly derived from ultraviolet photoemission spectroscopy measurements. Interface dipoles are found to form according to the electron affinities of the substrates and PTCDA films at the interfaces and, consequently, the vacuum level alignment rule does not hold. For vanishing interface dipole the lowest unoccupied molecular orbital of PTCDA is found to align with the conduction band minimum of GaAs resulting in electron affinity of 4.12 eV for PTCDA. This provides an energy gap in the range of 2.44–2.55 eV, which is larger than the onset of optical absorption. The same procedure is applied to DiMe-PTCDI layers.

(Some figures in this article are in colour only in the electronic version)

[5] Author to whom any correspondence should be addressed.

  

## 1. Introduction

Organic semiconductors have attracted increasing interest owing to their potential application in various electronic and opto-electronic devices. The progress in the development of organic molecular beam deposition (OMBD) has led to monolayer level control in the growth process of organic thin films under ultrahigh-vacuum (UHV) conditions [1]. One of the possible applications of ultrathin layers of organic molecules is the passivation of semiconductor surfaces, such as Si(111)-(7 × 7) and GaAs(100) [2]. For example, a $C_{60}$ monolayer on a Si(111)-(7 × 7) surface inhibits chemical attack by water and atmospheric oxygen [2]. Moreover, it was already demonstrated that the deposition of organic molecules, in particular, 3,4,9,10-perylenetetracarboxylic dianhydride (PTCDA), is useful to characterize the inorganic semiconductor surface state distribution [1].

The electronic structure of organic/inorganic interfaces depends strongly on the crystalline structure of the organic films and the interface bonding. These properties have been found to be determined by the substrate surface [3–11]. For III–V inorganic semiconductors, particularly GaAs(100) surfaces, various methods of surface treatment have been developed to improve the chemical and electronic properties of the surfaces. One of the most widely used methods for the passivation of the GaAs(100) surface is chalcogen passivation using S, Se, and Te atoms. Hirose *et al* [3, 4] investigated the initial growth of PTCDA molecules on various GaAs(100) surfaces using low-energy electron diffraction (LEED). The Se-passivated GaAs(100)-(2 × 1) surface results in PTCDA films with good crystallinity, whereas the deposition on the GaAs(100)-(2 × 4) or c(2 × 8) reconstructed surfaces produces films with crystallites randomly oriented in the plane parallel to the surface. The films grown on the GaAs(100)-c(4 × 4) surface show intermediate molecular ordering. The difference in the molecular ordering depends on the interaction between organic molecules relative to that between organic molecules and the substrate surfaces.

It has already been reported that by introducing organic layers of different thicknesses into a metal/III–V semiconductor Schottky contact the effective barrier height can be tuned, and that such devices are still applicable in the gigahertz frequency regime [12–15]. Ultimately it is anticipated that optimizing electronic properties at those interfaces will lead to a reduction in power consumption of the device by lowering the operating voltage. Crucial for the understanding of the $I$–$V$ characteristics of devices is information about the alignment of transport levels at the interfaces. The energy alignment of the valence band maximum (VBM) and the highest occupied molecular orbital (HOMO) of GaAs and organic semiconductor, respectively, may serve as a injection barrier for holes and can be easily determined using photoemission spectroscopy. Injection barriers for electrons, on the other hand, are due to energy offsets between the conduction band minimum (CBM) and lowest unoccupied molecular orbital (LUMO).

The 'band gap' of materials such as PTCDA or DiMe-PTCDI ($N$,$N'$-dimethyl-3,4,9,10-perylenetetracarboxylic diimide)—the molecular structures are shown in figure 2—is defined as the energy gap between the HOMO and the LUMO. The transport gap $E_{\mathrm{trans}} = E_{\mathrm{LUMO,trans}} - E_{\mathrm{HOMO,trans}}$, which is the minimum energy for the formation of a separated free electron and hole pair, is found to be considerably larger than the optical one involving exciton formation. The transport gap can be determined from the energy separation of the centres of mass of the HOMO and LUMO levels recorded by photoemission and inverse photoemission spectroscopy, respectively, and subtracting from this value the vibrational contribution and the difference between bulk and surface polarizations [18]. From optical absorption measurements the optical band gap $E_{\mathrm{opt}}$ of PTCDA and DiMe-PTCDI is determined as 2.2 and 2.14 eV, respectively, which is considerably smaller than the transport gap [16, 17]. The difference can

be approximated by $E_{opt} = E_{trans} - E_{exc}$ with $E_{exc}$ being the exciton energy in the organic layer of 1 eV. For the determination of the transport gap, Hill *et al* performed combined photoemission and inverse photoemission measurement on PTCDA films. Taking into account polarization effects at the surface and in the bulk of the organic film they estimated the transport gap to be $3.2 \pm 0.4$ eV [18]. Thus, modelling the carrier injection using the optical gap should result in dramatic failure.

Quite often the vacuum level alignment is used to determine the energy level alignment at interfaces. Here, it is assumed that the vacuum levels of the materials in contact align at the interface and the interface barrier heights can simply be calculated using the ionization potentials (IPs) and electron affinities (EA) of semiconducting materials and work functions of metallic materials. For metal–organic interfaces a conclusion that in general the vacuum levels do not align has been reached [11, 18, 19]. The difference in vacuum levels is attributed to interface dipoles. Another important issue is the occurrence of 'band-bending'-like electrostatic energy shift in organic layers. Such shift is observed in many metal/organic systems [20]. This shift is in most cases confined to a regime of only a few nanometres, which cannot be accounted for using the conventional band-bending theory of inorganic semiconductors. For organic/inorganic semiconductor interfaces, however, no systematic study has been performed on the energy level alignment and all the questions mentioned above remain unresolved. The energy level alignments for interfaces of PTCDA on GaAs(100) and copper-phthalocyanine (CuPc) and $N,N'$-diphenyl-$N,N'$-bis(1-naphthyl)-1,1′-biphenyl-4,4″-diamine (NPD) on InP(110) were reported by Hirose *et al* [3] and Chasse *et al* [21], respectively. In all cases the vacuum level alignment rule does not hold. Schlaf *et al* reported a band bending of 0.75 eV in PTCDA films grown on $SnS_2$ substrates [22].

Here, ultraviolet photoemission spectroscopy (UPS) studies of PTCDA and DiMe-PTCDI deposition on differently treated GaAs(100) surfaces are presented. The ionization energy of the substrate surfaces was systematically varied from $5.23 \pm 0.10$, 5.55–$5.92 \pm 0.10$, to $6.40 \pm 0.10$ eV for GaAs(100)-c$(4 \times 4)$, wet chemically S-passivated GaAs(100), and Se-passivated GaAs(100)-$(2 \times 1)$ surfaces, respectively.

## 2. Experimental details

For the chalcogen passivation of GaAs(100) two different techniques were used: exposure to a flux of chalcogen atoms under UHV conditions and wet chemical etching in sulfur-containing solutions. For the UHV treatment, homoepitaxial n-GaAs(100) layers with a doping concentration of $N = 1 \times 10^{18}$ cm$^{-3}$ served as substrates. After their growth by molecular beam epitaxy they were covered by a thick amorphous arsenic layer to protect the GaAs(100) surfaces against contamination and oxidation. These samples were transferred into an UHV system with a base pressure of $p < 2 \times 10^{-8}$ Pa. The arsenic layer was then removed by gentle annealing to 380 °C. This leads to an As-rich c$(4 \times 4)$ or c$(2 \times 4)$ surface reconstruction of the GaAs(100) surface as can be judged from the lineshape analysis of the measured photoemission spectra and additional LEED experiments. For the passivation under UHV conditions, $SnSe_2$ was used as the source material. This compound decomposes at 340 °C according to $SnSe_2 \rightarrow SnSe + Se\uparrow$ [23]. Selenium was evaporated onto the substrates kept at 330 °C. This treatment leads to a sharp $(2 \times 1)$ LEED pattern in agreement with the reconstruction observed previously [24–27]. For the wet chemical sulfur passivation, samples were first degreased and then etched in a 3:1 mixture of $CCl_4$ and $S_2Cl_2$ for 10 s. The etching was followed by rinsing of the samples successively in $CCl_4$, acetone, ethanol, and deionized water for 5 s each. After the samples had been transferred into a UHV system they

were annealed at 430 °C. It should be mentioned that the LEED patterns for the S-passivated surfaces vary from a (1 × 1) to a weak (2 × 1) reconstruction.

PTCDA (Lancaster) or DiMe-PTCDI (Syntec GmbH) were purified by vacuum sublimation. The organic materials were deposited under UHV conditions onto the modified GaAs surfaces with the thickness controlled by a quartz microbalance located in the vicinity of the sample. After each modification step, photoelectron spectra were taken from the valence band and Ga 3d, As 3d, Se 3d, and S 2p core levels. The measurements were performed under UHV conditions at a base pressure of $1 \times 10^{-8}$ Pa. Photoemission spectra were taken at BESSY using TGM2, U125, and RGBL monochromators with typical overall resolution (light–electrons) of 150 meV (300 meV for the TGM2). The photon energy was chosen for recording the core level emissions under surface-sensitive conditions. Valence band spectra were taken in another UHV system in Chemnitz, which is composed of a preparation chamber for the organic deposition and an analysis chamber equipped with an angle-resolved UPS system (VG ARUPS 10, base pressure $3 \times 10^{-10}$ mbar) and a He discharge lamp ($h\nu = 21.22$ eV). The overall resolution measured from the Fermi edge of polycrystalline Ag(111) is 0.15 eV. For both cases, a sample bias of −9 V was applied to the sample to determine the sample work function.

## 3. Results and discussion

### *3.1. Initial adsorption PTCDA and DiMe-PTCDI molecules on GaAs surfaces*

The interaction of PTCDA and DiMe-PTCDI was investigated by recording core level emission using soft x-ray radiation. The formation of covalent or ionic bonds should result in chemically shifted components where the shift in binding energy corresponds to the ionicity of the bond. For a detailed evaluation, the photoelectron core level spectra were curve fitted assuming Voigt profiles—a Lorentzian convoluted with a Gaussian lineshape—and using a non-linear least-squares fitting routine. While the Lorentzian lineshape is the natural broadening due to the finite lifetime of the core hole, the Gaussian broadening accounts for the instrumental resolution and also for any broadening due to disorder and potential variations across the surface [28]. The latter in particular occurs as a result of defects on the surface and related inhomogeneous band bending.

During curve fitting, the Lorentzian linewidth, spin–orbit splitting, and branching ratio were kept fixed at values providing satisfactory results over an entire series of spectra. These parameters are presented in table 1. The peak intensity, position, and Gaussian linewidth were variable. All binding energies are given for the $d_{5/2}$ components of the spin–orbit split core levels relative to the Fermi level. The Se 3d and S 2p core level spectra for the Se- and S-passivated surfaces shown in figure 1 are very similar in lineshape. The best fit for the spectra was obtained using two components. Pashley and Li [24] proposed a structural model for the Se-passivated GaAs(100) surface on the basis of STM, XPS results, and the electron counting rule. Assuming this structural model, the Se1 component at a binding energy of 55.3 eV is assigned to the emission from the Se atoms in a topmost Se dimer layer while Se2 corresponds to those in a $Ga_2Se_3$-like environment between a second Ga layer and a fourth Ga layer with vacancies. The Se2 component is shifted by 0.93 eV towards lower binding energy. This assignment is in good agreement with previous results [25, 26], electronegativity considerations, and also the stronger reactivity of the Se1 atoms upon subsequent metal deposition. Gundel and Faschinger [29] presented another promising structure model which has been further supported by DFT LDA calculations by Benito *et al* [30, 31]. In this structure model the Se atoms do not form dimers on the surface and the second Ga layer

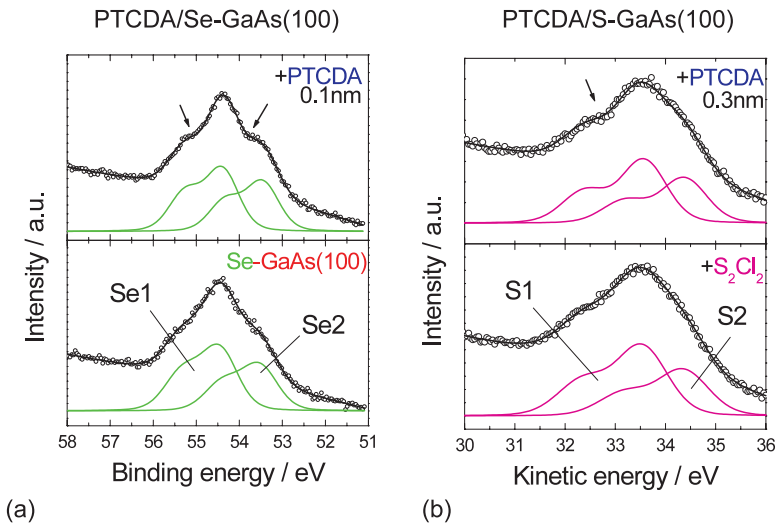


**Figure 1.** Se 3d and S 2p core level spectra (a) before and (b) after the deposition of PTCDA on chalcogen-passivated GaAs(100) surfaces.

**Table 1.** Fit parameters for the Ga 3d, As 3d, Se 3d, and S 2p core level spectra.

| Core level | Ga 3d | As 3d | Se 3d | S 2p |
|---|---|---|---|---|
| Lorentzian width ($eV^{-1}$) | 0.1 | 0.1 | 0.1 | 0.1 |
| Branching ratio | 1.58 | 1.50 | 1.60 | 2 |
| Spin–orbit splitting ($eV^{-1}$) | 0.48 | 0.68 | 0.86 | 1.18 |

is free of vacancies. Since the S 2p spectra have the same lineshape as the Se 3d spectra the structure model developed for the Se-passivated GaAs(100) surface can also be applied to the S-passivated GaAs(100) surface. Comparing the Ga 3d and the As 3d of Se- and S-passivated GaAs surfaces one will notice that the spectra from the S-passivated GaAs surface shown in figure 2 show two additional interface components, Ga3 and As2. The two interface components indicate that the As–S exchange reaction is less efficient than the As–Se exchange reaction, resulting in a less abrupt interface between the surface layer containing Ga and S and the GaAs bulk. This is supported by the fact that a higher temperature is necessary for the S passivation. Chalcogen-passivated GaAs surfaces are found to be chemically stable since they withstand considerable exposure to air.

PTCDA deposition onto the Se- and S-passivated surfaces does not induce any dramatic change in lineshape of the Se 3d and S 2p core level spectra, strongly indicating the absence of any chemical reaction of the PTCDA molecules with the Se- or S-terminated surfaces.

The intensity evolution of Ga 3d and As 3d bulk emission components with respect to the nominally deposited coverage indicates a Stranski–Krastanov-like growth mode, i.e. the formation of 1 ML (1 ML corresponds to 0.321 nm, which is the distance between the molecular planes in a PTCDA crystal and assuming flat-lying molecules) followed by island formation. From the exponential attenuation in the monolayer region the deposition rate was estimated to be 2 ML $min^{-1}$. The formation of islands can be attributed to the intermolecular interaction between PTCDA molecules being stronger than the interaction between the molecules and

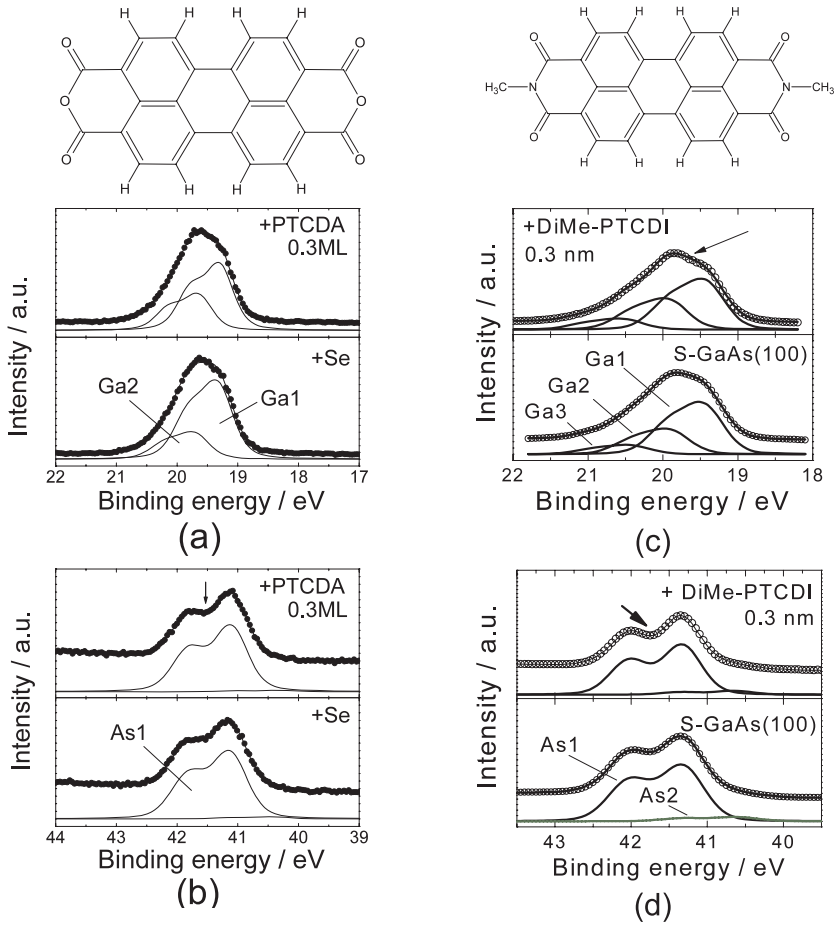


**Figure 2.** Molecular structures of PTCDA and DiMe-PTCDI. Ga 3d ((a), (c)) and As 3d ((b), (d)) core level spectra before and after the deposition of PTCDA and DiMe-PTCDI on Se- and S-passivated GaAs(100) surfaces, respectively.

the GaAs(100) surfaces, which is in contrast to epitaxial growth up to very thick films for PTCDA on alkali halides, such as NaCl(100) and KCl(100) [32, 33]. Comparing the results for PTCDA grown on S–GaAs(100), Se–GaAs(100), and GaAs(100)-c(4 × 4), island formation is most pronounced for PTCDA deposited on S–GaAs(100) and smallest for PTCDA grown on GaAs(100)-c(4 × 4).

However, a more subtle change is apparent, namely the shoulders at both sides of the peak become clearer (see arrows in figures 1(a), (b)). The curve fitting underlines this result more clearly. While the relative peak positions of the two components remain constant within an error of 10 meV, the Gaussian broadening of the Se 3d spectra changes from 0.87 to 0.78 eV by 90 meV. It should be pointed out that this decrease in Gaussian broadening was repeatedly observed upon PTCDA deposition onto Se-passivated GaAs(100) surfaces. Moreover, a very similar behaviour is found for the S 2p core level spectra during PTCDA deposition onto $S_2Cl_2$ wet chemically etched GaAs(100). At higher PTCDA coverage the Gaussian broadening remains constant. From the previous STM study [24, 34], it is known that a very well-ordered

Se-terminated (2 × 1) surface is produced by Se deposition and subsequent annealing. This study found that there are virtually no islands on any of the GaAs terraces in the STM image. However, there are still two types of defect on the surface observed: a few small holes assigned to missing dimers and many more small bright features. The density of these bright features is approximately $10^{12}$ cm$^{-2}$ in the image, which matches the density of dopant atoms on the surface at a doping concentration of (3–6) × $10^{18}$ cm$^{-3}$ used in that study. Our samples were treated in slightly different conditions. However, a sharp (2 × 1) LEED pattern was observed, confirming that the surface is also well reconstructed. At the doping level used in our experiments ($n = 1 \times 10^{18}$ cm$^{-3}$), the number of dopant atoms on the surface would also be $\sim 10^{12}$ cm$^{-2}$ among $6 \times 10^{14}$ cm$^{-2}$ surface atoms. This means that there is approximately one dopant atom in 300 surface unit cells.

It is also well known that the PTCDA molecules preferentially adsorb on defect sites due to an enhanced interaction [1, 35]. Certainly, 0.3 ML PTCDA are sufficient to cover all defect sites induced by dopant atoms. Indeed no more change is observed in the Gaussian broadening upon further PTCDA deposition. Hence, the sharpening of the core level spectra being indicative of a removal of inhomogeneous pinning is attributed to the preferential adsorption of PTCDA on the defect sites. Since the Si dopant atoms have a relatively small covalent radius (1.11 Å), they may induce local distortion of the surface. Upon PTCDA deposition on top of the dopant atoms, Si atoms may undergo geometrical relaxation accompanied by charge redistribution, resulting in a more homogeneous surface. However, charge transfer may also occur via a chemical reaction of the PTCDA with the defect sites. While the lineshape of the Se 3d core level spectra does not reveal any evidence for covalent bonding between PTCDA and the Se or S atoms, we cannot exclude the possibility of a reaction with dopant atoms. The latter is not detectable due to the low defect density. In addition, PTCDA is a non-polar molecule due to its mirror symmetry, which annihilates local dipole moments of polar carboxylic and anhydride groups. However, electric fields induced by the local dipole moment of the side groups and the van der Waals force of the whole molecule may also influence the charge redistribution at the interface.

The influence of the organic molecules on the core level spectra of deeper-lying Ga and As atoms is less pronounced. The results are presented in figure 2. For instance, the As 3d core level spectra seem to be sharper upon PTCDA deposition as can be judged from a slightly deeper dip between the spin–orbit split components (see the arrows in figures 2(a), (b)). Values derived from curve fitting for the decrease in Gaussian broadening are in the order of tens of millielectronvolts. Such an effect clearly requires further confirmation using higher-resolution experiments. There are two dominant components found in the Ga 3d core level spectra. From angle-dependent photoemission spectra [26], Ga2 is assigned to the Ga layer below Se surface atoms while Ga1 corresponds to bulk Ga atoms. Upon 0.3 ML PTCDA deposition the overall lineshape of Ga 3d core level spectra hardly changes. However, curve fitting results seem to indicate an increasing contribution of the subsurface Ga2 component. The initial stage of PTCDA deposition on defect sites may thus also influence subsurface Ga layers. This effect was repeatedly observed in all samples.

A similar behaviour is found for the adsorption of DiMe-PTCDI on S-passivated GaAs(100). Unfortunately, only the Ga 3d and As 3d core level emission could be investigated. The resolution and intensity of the set-up used for this investigation was not sufficient for investigating the S 2p core level. Following the deposition of a thin DiMe-PTCDI layer the As 3d Ga 3d core levels show the same behaviour as upon PTCDA deposition (see the arrows in figures 2(c), (d)), i.e. a decrease in linewidth of 10 and 70 meV for the Ga 3d and As 3d core levels, respectively. This favours the conclusion that DiMe-PTCDI decreases inhomogeneous Fermi level pinning on GaAs surfaces.

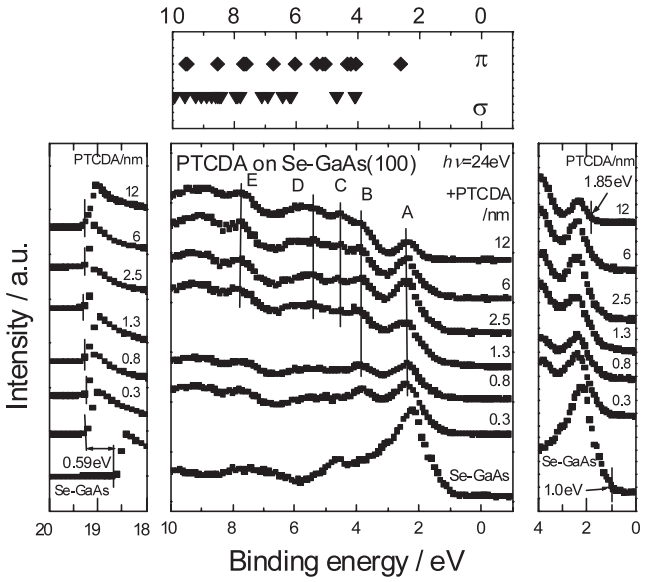


**Figure 3.** Valence band spectra of PTCDA deposited on Se–GaAs for several thicknesses. The upper panel shows calculated energy positions of occupied $\pi$- and $\sigma$-orbitals. The spectra were measured with synchrotron radiation of $h\nu = 24$ eV.

### *3.2. Energy level alignment at PTCDA/GaAs interfaces*

Figure 3 shows UP spectra for the clean Se–GaAs(100) surface and after subsequent stepwise deposition of a 12 nm PTCDA film onto this surface. In the spectra of a thick PTCDA films, five features labelled A, B, C, D, and E are clearly seen. This is in good agreement with previous work [3, 36, 37]. For the assignment of the spectral features the experimental data are compared to results from molecular orbital calculations using density functional theory. The calculations were performed using the Gaussian 98 package [38] at the B3LYP level of theory with a standard 6-31G(d) basis set. The energy levels of all molecular orbitals in the respective energy ranges are shown in the upper panel. To align the highest occupied energy level with centre of the lowest-binding-energy feature in the UP spectra all molecular orbitals were shifted by 0.65 eV to higher binding energies. The feature A with the lowest binding energy is attributed to the HOMO and originates from a molecular orbital which has a $\pi$-character and is distributed predominantly over the perylene core. The features B, C, and D have a predominant $\pi$-character, while predominantly $\sigma$-orbitals contribute to feature D.

The left and right panels show the onset of the high-binding-energy (low-kinetic-energy) secondary-electron peak and the valence band structures, respectively. The ionization energy of the substrate is obtained by subtracting the total width of the valence band spectra from the photon energy, i.e. $\mathrm{IP_S} = h\nu - (E_{\text{cut-off}} - E_{\mathrm{VBM}})$. Here, $E_{\text{cut-off}}$ and $E_{\mathrm{VBM}}$ represent the energy positions of the secondary-electron onset and the VBM of the substrate surfaces relative to $E_{\mathrm{F}}$, respectively.

$\mathrm{IP_{PTCDA}}$ was obtained by replacing $E_{\mathrm{VBM}}$ by the low-binding-energy edge of the HOMO ($E_{\mathrm{HOMO}}$) in the previous equation. The energy position is determined from the intercept of two linear extrapolations, one describing the background and the second one from the low-binding-energy region in the HOMO peak, tangent to the curve at the inflection point. The shifts in $E_{\text{cut-off}}$ upon PTCDA deposition can be interpreted as interface dipoles while the

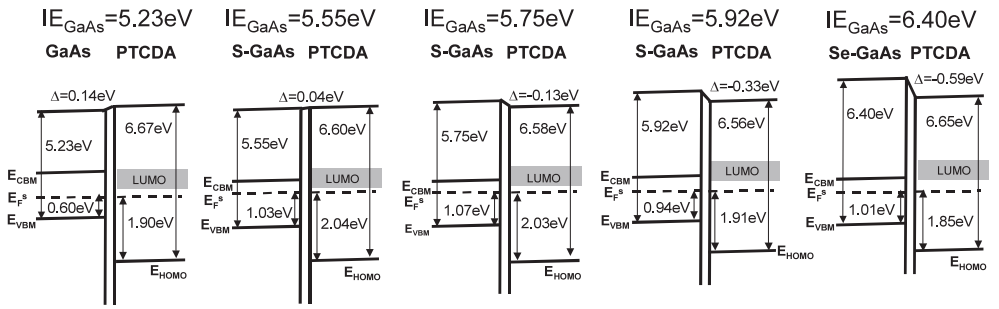


**Figure 4.** Energy level alignment at interfaces of PTCDA on GaAs(100) surfaces with different IPs. The shaded region represents the possible energy position range of the LUMO. The lower and upper limits are drawn considering the optical (2.2 eV) and transport HOMO–LUMO gaps (2.8 eV) of the PTCDA. The transport gap was obtained by adding an energy difference of 0.6 eV between the optical and transport gaps.

energy barrier for hole transport is obtained from $E_{\mathrm{VBM}} - E_{\mathrm{HOMO}}$. The only energy positions that are not directly obtained from the measured UP spectra are $E_{\mathrm{CBM}}$ for the substrates and $E_{\mathrm{LUMO}}$ for the PTCDA films. In order to determine $E_{\mathrm{CBM}}$ it is reasonable to use the optical gap (1.42 eV) because of the low polarization energies and high carrier screening efficiency leading to exciton binding energies of a few millielectronvolts [18]. This optical gap of GaAs(100) does not change upon using different surface treatment since the modification is confined within a few atomic layers. On the other hand, $E_{\mathrm{LUMO}}$ for the PTCDA film is not well known. The difference between the optical and transport HOMO–LUMO gaps of PTCDA films were proposed by Hill *et al* using UPS and inverse photoemission [1, 18]. This value amounts to $\sim$0.6 eV. The accuracy of this value, however, is limited by the rather poor resolution of inverse PS.

Figure 4 shows the energy level alignment obtained from UP spectra between PTCDA films and GaAs(100) surfaces with different IPs. For simplicity, the band bending of the substrates is omitted, so the energy level positions corresponding to the substrates represent those of the substrate surfaces. It can be seen that the different surface treatment varies the IPs of the GaAs(100) surfaces. The measured IPs range from $5.23 \pm 0.10$ eV for the GaAs(100)-c($4 \times 4$), 5.55–$5.92 \pm 0.10$ eV for S–GaAs(100), to $6.40 \pm 0.10$ eV for the Se–GaAs(100) surfaces. The IPs of the GaAs(100)-c($4 \times 4$) surface agree well with the value of 5.29 eV reported previously [39]. It is known that the passivation of GaAs(100) surfaces by S or Se atoms terminates the chemically active sites, leading to the formation of S–Ga or Se–Ga surface dipoles with S or Se atoms on the surfaces, and thus inducing the change in the IPs. It should be noted that the scatter of the IPs observed for S–GaAs(100) surfaces can be correlated with the development of the VB structures. A slightly different temperature ramp rate and pressure increase during annealing appears to strongly affect the degree of the related surface reconstruction. On these surfaces, PTCDA was evaporated in a stepwise manner. The energy levels of the PTCDA films were obtained using the UP spectra of thin (4–12 nm) PTCDA films in order to prevent any influence due to sample charging.

The energy position corresponding to the centre of the PTCDA HOMO in UP spectra for each sample does not appear to change during the stepwise deposition despite the fact that it is difficult to evaluate the energy shift below a PTCDA thickness of 1 nm due to the screening by the VB features of the substrates. This indicates that the PTCDA films show no 'band-bending'-like behaviour. The measured $\mathrm{IP}_{\mathrm{PTCDA}}$ fluctuates slightly from 6.56 to 6.67 eV, probably due to slight variations in surface morphology and molecular orientation [19]. However, the values

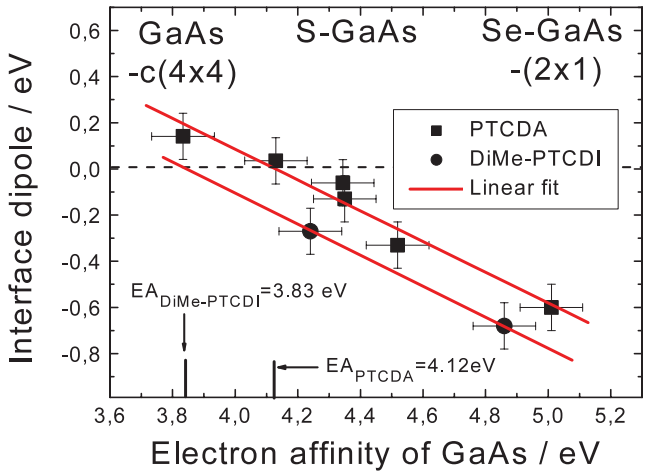


**Figure 5.** The interface dipole formed at PTCDA/GaAs(100) interfaces versus the electron affinity of GaAs(100) substrate surfaces.

are still within the error of the measurements (±0.1 eV). $E_{\mathrm{HOMO}}$ is found to be in the range of 1.85–2.04 eV, showing a weak dependence on the IPs. This indicates that the ability of $E_{\mathrm{F}}$ to move within the HOMO–LUMO gap is low. A pinning of the Fermi level was also observed for PTCDA/metal interfaces [19]. The shaded region in figure 4 shows the possible energy position range for the PTCDA LUMO, with the lower limit being drawn using the optical HOMO–LUMO gap value of PTCDA (2.2 eV) obtained from the energy position of the first peak in the optical absorption spectra of PTCDA films. The upper limit is obtained considering an energy difference of 0.6 eV between the optical and transport HOMO–LUMO gaps of PTCDA [18].

A strong correlation is found between the interface dipole and the relative energy position of $E_{\mathrm{LUMO}}$ and $E_{\mathrm{CBM}}$ and, respectively, the EA of the PTCDA film ($\mathrm{EA_{PTCDA}}$) and that of the substrates ($\mathrm{EA_S}$). $E_{\mathrm{HOMO}}$ is always located well below $E_{\mathrm{VBM}}$. At the PTCDA/GaAs(100)-c(4 × 4) interface where a positive interface dipole is formed, $E_{\mathrm{LUMO}}$ is located below $E_{\mathrm{CBM}}$. The situation is reversed when a negative dipole is formed, as in the case of the PTCDA/Se–GaAs(100) interface. Consequently, the interface dipole formed at the PTCDA/S–GaAs(100) interface varies from positive to negative depending on the IPs (or $\mathrm{EA_S}$). It can therefore be deduced that the formation of the interface dipole at PTCDA/GaAs(100) interfaces is possibly driven by the difference of $\mathrm{EA_S}$ and $\mathrm{EA_{PTCDA}}$ and that in general the vacuum level alignment rule is not applicable for those interfaces. At thermal equilibrium, the number of electrons and holes that are transported across the interfaces should be equal. Due to the difference in EA and IP between substrate surfaces and PTCDA films, each electron and hole transported undergoes an energy loss or gain. The net energy loss, therefore, depends on the electron and hole concentration that is transported across the interface and the energy difference of $\mathrm{EA_S} - \mathrm{EA_{PTCDA}}$ and $\mathrm{IP_S} - \mathrm{IP_{PTCDA}}$. The interface dipole is formed in order to compensate for the net energy loss. In the case of PTCDA films on n-GaAs(100) surfaces, the number of electrons transported across the interface is expected to be much higher than that of holes and, therefore, $\mathrm{EA_S} - \mathrm{EA_{PTCDA}}$ can be proposed to be the determining driving force for the interface dipole formation.

In figure 5 the interface dipole is presented as a function of $\mathrm{EA_S}$. It can be seen that the interface dipole formed at PTCDA/GaAs(100) interfaces is linearly dependent on $\mathrm{EA_S}$.

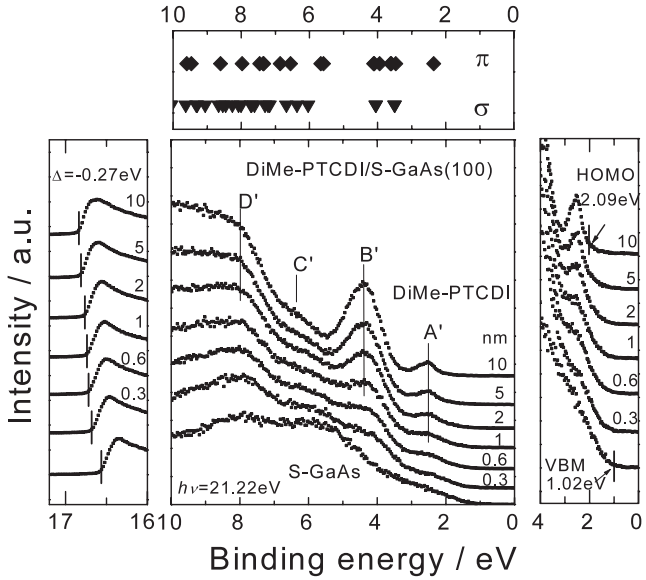


**Figure 6.** Valence band spectra of DiMe-PTCDI deposited on S–GaAs for several thicknesses. The upper panel shows calculated energy positions of occupied $\pi$- and $\sigma$-orbitals. The spectra were measured with a He discharge lamp ($h\nu = 21.2$ eV).

Using a linear fit, the interface dipole is found to be zero at $EA_S = 4.12 \pm 0.10$ eV. This value also represents $EA_{PTCDA}$, assuming that the formation of the interface dipole is driven by the difference of $EA_S$ and $EA_{PTCDA}$. Using $EA_{PTCDA} = 4.12 \pm 0.10$ eV, the energy offset between $E_{CBM}$ and $E_{LUMO}$ at the interfaces can be estimated to be $-0.17 \pm 0.10$ eV for PTCDA/GaAs(100)-c(4 × 4), 0.05–0.087 ± 0.10 eV for PTCDA/S–GaAs(100), and $0.27 \pm 0.10$ eV for PTCDA/Se–GaAs(100) interfaces. In addition, assuming that the energy level of the PTCDA films extends up to the interfaces without energy shifts, we can estimate the HOMO–LUMO gap to be in the range of 2.44–2.55 eV. This value is larger than the optical gap of PTCDA but still smaller than the transport HOMO–LUMO gap proposed by Hill *et al* [18].

Comparable UPS spectra for the growth of DiMe-PTCDI on S-passivated GaAs(100) are shown in figure 6. As for PTCDA, the HOMO consists of a single $\pi$-orbital. The major difference in the UP spectra from PTCDA and DiMe-PTCDI is the strong peak at a binding energy of ∼4.5 eV in the spectrum of DiMe-PTCDI. This peak is characteristic for DiMe-PTCDI and stems from the $\pi$- and $\sigma$-bonds located at the imide, carboxyl, and methyl groups of the molecule.

For the clean substrate surface the position of the VBM in S–GaAs is found at $1.02 \pm 0.10$ eV with respect to the Fermi level $E_F$, while the ionization is determined as $5.66 \pm 0.10$ eV. The evolution of the spectra with increasing DiMe-PTCDI deposition reveals that there is no detectable change in band bending in the GaAs substrate. The DiMe-PTCDI HOMO does not change its energy position as a function of the film thickness. As in the case of PTCDA films grown on Se-passivated GaAs(100) surfaces, there is no indication for a 'band-bending'-like behaviour in DiMe-PTCDI. After 10 nm of DiMe-PTCDI has been deposited the HOMO position is $2.09 \pm 0.10$ eV relative to $E_F$. Therefore the HOMO is located $1.07 \pm 0.10$ eV below the VBM. Moreover, the formation of an interface dipole can be derived from the shift of the secondary-electron cut-off at high binding energy (see the left panel of figure 1). Here, there is a slow evolution of the low-energy cut-off with coverage

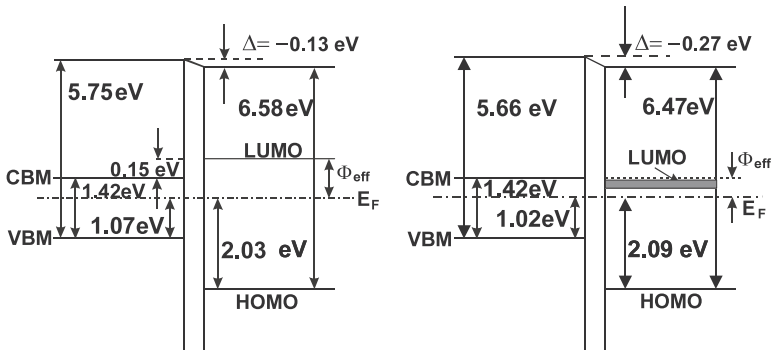


**Figure 7.** Energy level alignment at the interface between S–GaAs(100) and PTCDA (left) and DiMe-PTCDI (right).

while in figure 3 there is a rapid shift for the lowest coverage. This different behaviour is due to different growth modes of the organic materials on S-passivated GaAs(100). While the growth of PTCDA follows the Stranski–Krastanov mode, the growth of DiMe-PTCDI seems to start immediately with the formation of islands. For a nominal coverage of 0.3 nm, PTCDA has formed a monolayer and covers the whole substrate surface, while DiMe-PTCDI covers only a part of the substrate surface.

With the interface dipole of $\Delta = -0.27 \pm 0.10$ eV and the HOMO position, the energy level alignment diagram at the DiMe-PTCDI/S–GaAs(100) interface is determined and presented in figure 7 in comparison with the energy level alignment of the PTCDA/S–GaAs(100) interface. For another sample the ionization energy of the substrate was determined as $6.28 \pm 0.10$ eV which is close to the value for Se-passivated GaAs(100) samples. On this substrate the interface dipole amounts to $\Delta = -0.68 \pm 0.10$ eV which is larger than for the PTCDA/Se–GaAs(100) interface. The data for these two samples are also presented in figure 5. A least-squares fit to the data gives an electron affinity for DiMe-PTCDI of $3.86 \pm 0.10$ eV. With the ionization energy of $6.46 \pm 0.10$ eV a transport gap of $2.6 \pm 0.10$ eV is determined.

For further discussion it is worth having a look at the optical gaps determined from the position of the first peak in optical absorption and the exciton binding energies. The values are 2.22 and 2.14 eV for PTCDA and DiMe-PTCDI, respectively [16, 17]. On the other hand, the exciton binding energy of an organic solid is known to depend on the crystalline structure [40]. While the x-ray diffraction spectrum of the 10 nm PTCDA film shows a peak corresponding to (102) direction, no peak is revealed on even thicker DiMe-PTCDI films. Consequently, the exciton binding energy of the DiMe-PTCDI film is expected to be considerably larger than that of the PTCDA film ($\sim$0.6 eV), giving rise to a larger transport gap of the DiMe-PTCDI film. However, a short-range order still exists in the DiMe-PTCDI film as can be seen in several intermolecular vibration modes in the Raman spectrum [41]. Nevertheless a smaller IE and a larger transport gap of the DiMe-PTCDI will result in a smaller EA for DiMe-PTCDI, which is in good agreement with the experimental results. However, the LUMO of DiMe-PTCDI should be located above $E_{\mathrm{CBM}}$, which is in contradiction with our $I$–$V$ measurements on Ag/DiMe-PTCDI/GaAs(100) samples [42]. These measurements indicate that the LUMO is at or below the CBM of GaAs and that the transport gap amounts to $2.42 \pm 0.10$ eV. Taking into account the experimental error of $\pm 0.10$ eV, the transport gaps determined by UP and $I$–$V$ measurements are still in agreement, but additional UP and $I$–$V$ measurements on DiMe-PTCDI grown on non-passivated GaAs(100) substrates will be performed to clarify this point.

It is so far not known how much of $\Delta$EA will contribute to the resulting interface dipole. As discussed, it is not only $\Delta$EA that determines the interface dipole. The free carrier type and density and the ability of organic molecules to transfer the charge within the layer can also have an influence. However, by simply adding the differences in $E_{\mathrm{opt}}$ (0.06 eV) and the interface dipole (0.12 eV) at the two interfaces, it can roughly be estimated that the exciton binding energy within the DiMe-PTCDI film is $\sim$0.2 eV larger than that within the PTCDA film.

## 4. Conclusions

PTCDA and DiMe-PTCDI molecules evaporated on GaAs(100) surfaces are found to adsorb preferentially on defect sites, thus inducing a reduction of inhomogeneous Fermi level pinning on the substrate surface. Depending on the substrate treatment, the IPs of the GaAs surfaces vary from $5.23 \pm 0.10$ to $6.40 \pm 0.10$ eV. An interface dipole is found to form according to the difference $\mathrm{EA_S} - \mathrm{EA_{PTCDA}}$ at the interfaces and the vacuum level alignment rule is not valid for such interfaces. The electron affinity for PTCDA which was obtained at zero interface dipole from a linear fit of the interface dipole versus $\mathrm{EA_S}$ is $4.12 \pm 0.10$ eV and, using this value, the energy offset between $E_{\mathrm{CBM}}$ and $E_{\mathrm{LUMO}}$ at the interfaces was estimated. The HOMO–LUMO gap of 2.44–2.55 eV is in agreement with the lower limit estimated from the electrical measurements. For DiMe-PTCDI grown on S–GaAs(100) the offset between the HOMO and VBM is 100 meV larger than for the PTCDA/S–GaAs(100) interface. The transport gap of DiMe-PTCDI is determined as $\sim$2.6 eV.

## Acknowledgments

We are grateful to the Bundesministerium für Bildung und Forschung (BMBF, No 05 SE8OCA 7) and the EU-funded Human Potential Research Training Network 'DIODE' (Contract No: HPRN-CT-1999–00164) for financial support. We also would like to thank Freiberger Compound Materials for their support and Professor Antoine Kahn for fruitful discussions.

## References

[1] Forrest S R 1997 *Chem. Rev.* **97** 1793
[2] Dunn A W, Moriarty P, Upward M D and Beton P H 1996 *Appl. Phys. Lett.* **69** 506
[3] Hirose Y, Chen W, Haskal E I, Forrest S R and Kahn A 1994 *Appl. Phys. Lett.* **64** 3482
[4] Hirose Y, Forrest S R and Kahn A 1995 *Phys. Rev.* B **52** 14040
[5] Hirose Y, Forrest S R and Kahn A 1995 *Appl. Phys. Lett.* **66** 944
[6] Kendrick C and Kahn A 1998 *Surf. Rev. Lett.* **5** 289
[7] Glöckler K, Seidel C, Soukopp A, Sokolowski M, Umbach E, Böhringer M, Berndt R and Schneider W-D 1998 *Surf. Sci.* **405** 1
[8] Stahl U, Gador D, Soukopp A, Fink R and Umbach E 1998 *Surf. Sci.* **414** 423
[9] Taborski J, Väterlein P, Dietz H, Zimmermann U and Umbach E 1995 *J. Electron Spectrosc. Relat. Phenom.* **75** 129
[10] Chizhov I, Kahn A and Scoles G 2000 *J. Cryst. Growth* **208** 449
[11] Ishii H, Sugiyama K, Ito E and Seki K 1999 *Adv. Mater.* **11** 605
[12] Böhler A, Urbach P, Ammermann D and Kowalsky W 1998 *Mater. Sci. Eng.* B **51** 58
[13] Kampen T U, Park S and Zahn D R T 2002 *Appl. Surf. Sci.* **190** 461
[14] Forrest S R, Kaplan M L, Schmidt P H and Parsey J M Jr 1985 *J. Appl. Phys.* **58** 867
[15] Forrest S R, Kaplan M L and Schmidt P H 1984 *J. Appl. Phys.* **55** 1492
[16] Kaiser R, Friedrich M, Schmitz-Hübsch T, Sellam F, Kampen T U, Leo K, Zahn D R T and Fresenius 1999 *J. Anal. Chem.* **363** 189
[17] Bulovic V, Burrows P E, Forrest S R, Cronin J A and Thompson M E 1996 *Chem. Phys.* **210** 1
[18] Hill I G, Kahn A, Soos Z G and Pascal R A Jr 2000 *Chem. Phys. Lett.* **327** 181

[19] Hill I G, Rajagopal A, Kahn A and Hu Y 1998 *Appl. Phys. Lett.* **73** 662
[20] Hill I G, Makinen A J and Kafa Z H 2000 *Appl. Phys. Lett.* **77** 1825
[21] Chasse T, Wu C I, Hill I G and Kahn A 1999 *J. Appl. Phys.* **85** 6589
[22] Schlaf R, Schroeder P G, Nelson N W, Parkinson B A, Lee P A, Nebesny K W and Armstrong N R 1999 *Phys. Rev.* B **86** 1499
[23] Li Z S, Cai W Z, Su R Z, Dong G S, Huang D M, Ding X M, Hou X Y and Xun Wang 1994 *Appl. Phys. Lett.* **64** 3425
[24] Pashley M D and Li D 1994 *J. Vac. Sci. Technol.* A **12** 1848
[25] Hohenecker St, Drews D, Lubbe M, Zahn D R T and Braun W 1998 *Appl. Surf. Sci.* **123/124** 585
[26] Hohenecker St, Kampen T U, Zahn D R T and Braun W 1998 *J. Vac. Sci. Technol.* B **16** 2317
[27] Hohenecker St, Kampen T U, Werninghaus T, Zahn D R T and Braun W 2001 *Appl. Surf. Sci.* **175/176** 1658
[28] Moriarty P, Murphy B, Roberts L, Cafolla A A, Hughes G, Koenders L and Bailey P 1994 *Phys. Rev.* B **50** 14237
[29] Gundel S and Faschinger W 1999 *Phys. Rev.* B **59** 5602
[30] Kampen T U, Zahn D R T, Braun W, González C, Benito I, Ortega J, Jurczyszyn L, Blanco J M, Pérez R and Flores F 2003 *Appl. Surf. Sci.* **212/213** 850
[31] González C, Benito I, Ortega J, Jurczyszyn L, Blanco J M, Pérez R, Flores F, Kampen T U, Zahn D R T and Braun W 2003 *J. Phys.: Condens. Matter* submitted
[32] Forrest S R 1997 *Chem. Rev.* **97** 1793
[33] Mobus M, Karl N and Kobayashi T 1992 *J. Cryst. Growth* **116** 495
[34] Li D and Pashley M D 1994 *Phys. Rev.* B **49** 13643
[35] Park S, Kampen T U, Braun W and Zahn D R T 2000 *Appl. Phys. Lett.* **76** 3200
[36] Azuma Y, Akatsuka S, Okudaira K K, Harada Y and Ueno N 2000 *J. Appl. Phys.* **87** 766
[37] Kera S, Setoyama H, Onoue M, Okudaira K K, Harada Y and Ueno N 2001 *Phys. Rev.* B **63** 15204
[38] Frisch M J, Trucks G W, Schlegel H B, Scuseria G E, Robb M A, Cheeseman J R, Zakrzewski V G, Montgomery J A, Stratmann R E, Burant J C, Dapprich S, Millam J M, Daniels A D, Kudin K N, Strain M C, Farkas O, Tomasi J, Barone V, Cossi M, Cammi R, Mennucci B, Pomelli C, Adamo C, Clifford S, Ochterski J, Petersson G A, Ayala P Y, Cui Q, Morokuma K, Malick D K, Rabuck A D, Raghavachari K, Foresman J B, Cioslowski J, Ortiz J V, Stefanov B B, Liu G, Liashenko A, Piskorz P, Komaromi I, Gomperts R, Martin R L, Fox D J, Keith T, Al-Laham M A, Peng C Y, Nanayakkara A, González C, Challacombe M, Gill P M W, Johnson B G, Chen W, Wong M W, Andres J L, Head-Gordon M, Replogle E S and Pople J A 1998 *Gaussian 98 (Revision A.1)* (Pittsburgh, PA: Gaussian)
[39] Hirose K, Foxman E, Noguchi T and Uda M 1990 *Phys. Rev.* B **41** 6076
[40] Hill I G, Kahn A, Soos Z G and Pascal R A Jr 2000 *Chem. Phys. Lett.* **327** 181
[41] Salvan G, Park S, Kampen T U and Zahn D R T 2003 unpublished
[42] Zahn D R T, Kampen T U and Méndez H 2003 *Appl. Surf. Sci.* **212/213** 423